Ultrashort stretched-pulse L-band laser using carbon-nanotube saturable absorber

Won Sik Kwon,[1]Hyub Lee,[1]Jin Hwan Kim,[1]Jindoo Choi,[1] Kyung-Soo Kim,[1,2] and Soohyun Kim[1,*]

[1]*Division of Mechanical Engineering, Korea Advanced Institute of Science and Technology, Daejeon 305-701, South Korea*

[2]*kyungsookim@kaist.ac.kr*

[*]*soohyun@kaist.ac.kr*

Abstract: In the paper, a passively mode-locked erbium-doped fiber ring laser in the long-wavelength band (L-band) is presented by using a single-wall nanotube saturable absorber (SWNT-SA). The optical properties of the SWNT-SA are compared with those in the C-band in view of the absorbance spectrum and the power-dependent transmittance of the SWNT-SA film. The effects of the net cavity dispersion and the length of the erbium-doped fiber (EDF) on L-band stretched pulse generation are discussed. The designed stretched-pulse L-band laser has a net dispersion of 0.017-ps^2 and generates ultrashort (110 fs), broad-spectrum (41 nm) pulses with a signal-to-noise ratio over 70 dB.

OCIS codes: (060.2320) Fiber optics amplifiers and oscillators; (320.7090) Ultrafast lasers.

References and links

1. U. Keller, "Recent developments in compact ultrafast lasers," Nature **424**(6950), 831–838 (2003).
2. M. E. Fermann and I. Hartl, "Ultrafast fiber laser technology," IEEE J. Sel. Top. Quantum Electron. **15**(1), 191–206 (2009).
3. T. Hasan, Z. Sun, F. Wang, F. Bonaccorso, P. H. Tan, A. G. Rozhin, and A. C. Ferrari, "Nanotube–polymer composites for ultrafast photonics," Adv. Mater. **21**(38-39), 3874–3899 (2009).
4. H. Kataura, Y. Kumazawa, Y. Maniwa, I. Umezu, S. Suzuki, Y. Ohtsuka, and Y. Achiba, "Optical properties of single-wall carbon nanotubes," Synth. Met. **103**(1–3), 2555–2558 (1999).
5. S. Y. Set, H. Yaguchi, Y. Tanaka, and M. Jablonski, "Ultrafast fiber pulsed lasers incorporating carbon nanotubes," IEEE J. Sel. Top. Quantum Electron. **10**(1), 137–146 (2004).
6. D. Popa, Z. Sun, T. Hasan, W. B. Cho, F. Wang, F. Torrisi, and A. C. Ferrari, "74-fs nanotube-mode-locked fiber laser," Appl. Phys. Lett. **101**(15), 153107 (2012).
7. Y. W. Song, S. Yamashita, C. S. Goh, and S. Y. Set, "Carbon nanotube mode lockers with enhanced nonlinearity via evanescent field interaction in d-shaped fibers," Opt. Lett. **32**(2), 148–150 (2007).
8. K. Kieu and M. Mansuripur, "Femtosecond laser pulse generation with a fiber taper embedded in carbon nanotube/polymer composite," Opt. Lett. **32**(15), 2242–2244 (2007).
9. Z. H. Yu, Y. G. Wang, X. Zhang, X. Z. Dong, J. R. Tian, and Y. R. Song, "A 66 fs highly stable single wall carbon nanotube mode locked fiber laser," Laser Phys. **24**(1), 015105 (2014).
10. H. Jeong, S. Y. Choi, F. Rotermund, Y. H. Cha, D. Y. Jeong, and D. I. Yeom, "All-fiber mode-locked laser oscillator with pulse energy of 34 nj using a single-walled carbon nanotube saturable absorber," Opt. Express **22**(19), 22667–22672 (2014).
11. Z. Sun, A. G. Rozhin, F. Wang, V. Scardaci, W. I. Milne, I. H. White, F. Hennrich, and A. C. Ferrari, "L-band ultrafast fiber laser mode locked by carbon nanotubes," Appl. Phys. Lett. **93**(6), 061114 (2008).
12. Z. G. Lu, J. R. Liu, P. J. Poole, S. Raymond, P. J. Barrios, D. Poitras, G. Pakulski, P. Grant, and D. Roy-Guay, "An l-band monolithic InAs/InP quantum dot mode-locked laser with femtosecond pulses," Opt. Express **17**(16), 13609–13614 (2009).
13. H. Zhang, Q. L. Bao, D. Y. Tang, L. M. Zhao, and K. Loh, "Large energy soliton erbium-doped fiber laser with a graphene-polymer composite mode locker," Appl. Phys. Lett. **95**(14), 141103 (2009).
14. J. Du, S. M. Zhang, H. F. Li, Y. C. Meng, X. L. Li, and Y. P. Hao, "L-band passively harmonic mode-locked fiber laser based on a graphene saturable absorber," Laser Phys. Lett. **9**(12), 896–900 (2012).
15. J. Q. Zhao, Y. Gwang, P. G. Yan, S. C. Ruan, G. L. Zhang, H. Q. Li, and Y. H. Tsang, "An l-band graphene-oxide mode-locked fiber laser delivering bright and dark pulses," Laser Phys. **23**(7), 075105 (2013).

#232601 - $15.00 USD Received 16 Jan 2015; revised 6 Mar 2015; accepted 6 Mar 2015; published 17 Mar 2015

16. H. Ahmad, A. Zulkifli, F. Muhammad, M. Zulkifli, K. Thambiratnam, and S. Harun, "Mode-locked l-band bismuth–erbium fiber laser using carbon nanotubes," Appl. Phys. B **115**(3), 407–412 (2014).
17. J. L. Luo, L. Li, Y. Q. Ge, X. X. Jin, D. Y. Tang, D. Y. Shen, S. M. Zhang, and L. M. Zhao, "L-band femtosecond fiber laser mode locked by nonlinear polarization rotation," IEEE Photon. Technol. Lett. **26**(24), 2438–2441 (2014).
18. L. E. Nelson, D. J. Jones, K. Tamura, H. A. Haus, and E. P. Ippen, "Ultrashort-pulse fiber ring lasers," Appl. Phys. B. **65**(2), 277–294 (1997).
19. Y. Kimura and M. Nakazawa, "Lasing characteristics of er3+-doped silica fibers from 1553 up to 1603 nm," J. Appl. Phys. **64**(2), 516–520 (1988).
20. G. R. Lin, J. Y. Chang, Y. S. Liao, and H. H. Lu, "L-band erbium-doped fiber laser with coupling-ratio controlled wavelength tunability," Opt. Express **14**(21), 9743–9749 (2006).
21. P. Nikolaev, M. J. Bronikowski, R. K. Bradley, F. Rohmund, D. T. Colbert, K. A. Smith, and R. E. Smalley, "Gas-phase catalytic growth of single-walled carbon nanotubes from carbon monoxide," Chem. Phys. Lett. **313**(1–2), 91–97 (1999).
22. N. Nishizawa, Y. Nozaki, E. Itoga, H. Kataura, and Y. Sakakibara, "Dispersion-managed, high-power, er-doped ultrashort-pulse fiber laser using carbon-nanotube polyimide film," Opt. Express **19**(22), 21874–21879 (2011).
23. K. Kieu and F. W. Wise, "Self-similar and stretched-pulse operation of erbium-doped fiber lasers with carbon nanotubes saturable absorber," in *Conference on Lasers and Electro-Optics*, (Optical Society of America, 2009), paper CML3.
24. H. H. Liu and K. K. Chow, "Enhanced stability of dispersion-managed mode-locked fiber lasers with near-zero net cavity dispersion by high-contrast saturable absorbers," Opt. Lett. **39**(1), 150–153 (2014).
25. F. A. Flood, "L-band erbium-doped fiber amplifiers," in *Proccedings ofOptical Fiber Communication Conference, 2000*, (IEEE, 2000), pp. 102–104.

1. Introduction

Because of their ability to provide ultrashort pulse durations and a broad spectrum, passively mode-locked lasers have received much attention in various fields of science and industry such as pump-probe spectroscopy, optical coherence tomography (OCT), terahertz time-domain spectroscopy (THz-TDS), telecommunications [1, 2], and etc. Furthermore, fiber lasers that are mode-locked by single-wall nanotube saturable absorbers (SWNT-SAs) exhibit distinct practical advantages including mechanical and environmental robustness, and polarization insensitivity. In literature, a compact and portable all-fiber mode-locked laser was developed by inserting an SWNT-SA film with a thickness of a few tens of micrometers between the laser oscillator fiber tips [3].

SWNTs exhibit a distinct nonlinear optical property in the near-infrared region (1.2-2.0 μm), in which the peak of the first absorption band is determined by the distribution of diameters of SWNTs [4, 5]. Most studies have been successfully conducted at the wavelength of approximately 1550 nm, which is called the conventional wavelength band (C-band). To date, dramatic improvements in pulse width, spectrum bandwidth, and acquisition power have been demonstrated in the C-band. Popa et al. designed a stretched pulse laser mode-locked by an SWNT-SA film and successfully generated a pulse with a 74-fs duration and 63-nm bandwidth [6]. Moreover, application of SWNT-SAs to evanescent field absorption via a D-shaped fiber was first proposed by Song et al. to overcome the limitation of the optical damage threshold [7]. Tapered fiber and microfiber design based on evanescent field interactions were used to yield lasers which generate high-power and short-duration pulses [8–10].

Recently, there has been increasing interest in ultrashort pulse generation at the wavelength of approximately 1600 nm known as the long-wavelength band (L-band), where the light can propagate through the optical fiber with very high efficiency [11–17].The L-band is widely used in communication systems because the dense-wavelength-division-multiplexed (DWDM) systems that combine the C-band and L-band can increase the transmission capacity. Furthermore, the different spectral region of the L-band itself can contribute to further spectroscopic applications. The first demonstration of L-band pulse generation via SWN-SAs was performed in the soliton mode-locking regime [11]. In that work, the carbon nanotubes (CNTs) used were fabricated via laser ablation and had a 340-nm-wide absorption-band peak at 1600 nm. However, the pulse energy, spectral width and

#232601 - $15.00 USD Received 16 Jan 2015; revised 6 Mar 2015; accepted 6 Mar 2015; published 17 Mar 2015

pulse duration amounted to only 0.027 nJ, 5.7 nm, and ~498 ± 16 fs, respectively. These limited properties come from soliton mode-locking. In contrast, stretched-pulse lasers are an attractive type of laser that can generate pulses with high energy, large spectral width and low timing jitter [18]. Recently, L-band pulse generation was performed in the stretched-pulse regime using a bismuth-erbium fiber. The reported spectral width and pulse duration were 11.2 nm and 460 fs, respectively, which indicates improvement over the soliton mode-locking regime [16]. Despite these recent interests, reports on SWNT-SAs-based ultrafast pulse generation covering the L-band is rare and requires detailed analyses.

In this paper, we present an SWNT-SA mode-locked stretched-pulse laser design that yields a wide spectral width and short pulse duration in the L-band region. In the laser design, the length of the erbium-doped fiber (EDF) and nonlinear optical properties of the SWNT-SA are considered. The characteristics of the output pulse with respect to the EDF length and net cavity dispersion are investigated and discussed.

2. Experiment details

Figure 1 shows the configuration of the laser cavity. The EDF (ER80-4/125, LIKKIE) used in the laser has an 80 dB/m absorption peak at 1530 nm, and the EDF length and cavity loss affect the lasing wavelength [19, 20]. Given a cavity length L and the total cavity loss $\Gamma(\lambda)$, it holds that:

$$\max_{\lambda}\left\{g(\lambda)L+\frac{g(\lambda)+\alpha(\lambda)}{\alpha_p}\ln\left[\frac{P_p(L)}{P_p(0)}\right]-\ln\left[\Gamma_{TOT}(\lambda)\right]\right\}=0, \qquad (1)$$

where $g(\lambda)$, $\alpha(\lambda)$ and α_p denote the gain, attenuation and pumping absorption coefficients, respectively, and $P_p(z)$ is the pumping power [20]. Therefore, a longer central wavelength can be obtained by increasing the EDF length or decreasing the output coupling ratio to reduce the cavity loss. To enable L-band operation, we used an EDF length (1.5 m) that is longer than the conventionally used length for C-band operation (< 1 m). The output coupling ratio is 50:50 and maintained to avoid a reduction in the output power. To operate the fiber laser in the stretched-pulse mode-locked regime (in which the net dispersion of the cavity approaches zero), the lengths of the positively dispersive EDF and negatively dispersive SMF28 and HI1060 fibers are adjusted. The length of HI1060 flexcore with group velocity dispersion(GVD) of –0.007 ps^2/m at 1590 nm is fixed to 0.27 m and that of SMF28 (GVD of –0.026 ps^2/m at 1590 nm)varies from 0.77 m to 1.87 m. It should be noted that the EDF has a GVD of 0.031 ps^2/m at 1590 nm.

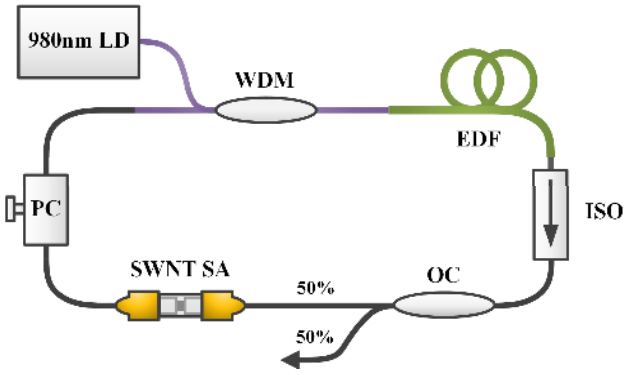

Fig. 1. Schematics of the fiber laser (LD:laser diode, WDF: wavelength division multiplexer, EDF: erbium-doped fiber, ISO: isolator, OC: optical coupler, PC: polarization controller).

#232601 - $15.00 USD Received 16 Jan 2015; revised 6 Mar 2015; accepted 6 Mar 2015; published 17 Mar 2015

We adopt the SWNTs which are produced by a high-pressure CO (HiPCO) disproportionation process [21] to fabricate an SWNT-sodium-carboxymethylcellulose (Na-CMC) composite film. The film is used as the SWNT-SA for passive mode-locking [3]. To compare the optical properties of the SWNT-SA in the L-band region with those in the C-band region, the absorbance spectrum and power-dependent transmittance of the SWNT-SA film are measured and shown in Fig. 2. Two laboratory-built femtosecond oscillators with similar pulse durations (~330 fs) and repetition rates (~60 MHz) but different central wavelengths (1560 and 1590 nm) are used to measure the power-dependent transmittance of the SWNT-SA. The peak absorption wavelength, decided by the mean diameter of the SWNT, corresponds to the first absorption band. As can be seen in Fig. 2(a), the SWNT-SA has a lower absorbance in the L-band than in the C-band. The fact that the absorbance level decreases when entering the L-band makes one expect degradation in the nonlinear characteristics of the SWNT film. Despite this lower absorption, in Fig. 2(b), the measured modulation depth in the L-band is ~10%, almost the same as that in the C-band. Thus, it may be seen that the SWNT-SA optical properties do not have a significant impact on mode locking in the L-band region. The SWNT/Na-CMC film is inserted between the fiber-channel angled-physical-contact (FC/APC) connectors following a 50:50 output coupler. The cavity is pumped using a 980-nm laser diode that emits in the forward direction. For a pumping power over 150 mW, a mode-locked pulse in the L-band region was generated.

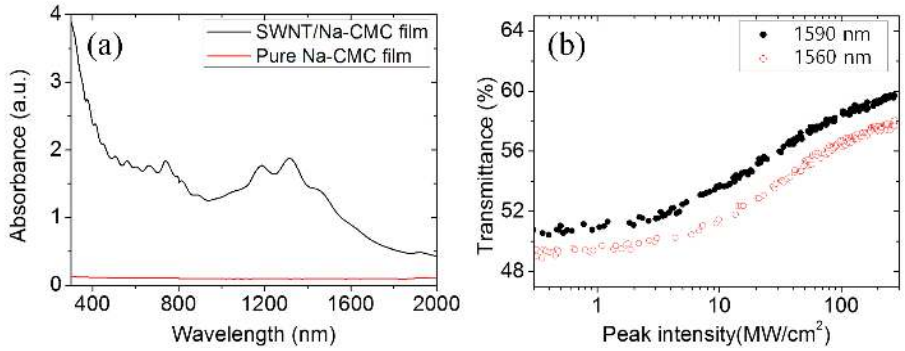

Fig. 2. Optical properties of the SWNT-SA: (a) Absorbance spectra of SWNT/NA-CMC and pure NA-CMC films (for SWNTs produced by the HiPCO process). (b) Power-dependent transmittance of an SWNT-SA film measured at 1560 nm (red) and 1590 nm (black).

We examined the net cavity dispersion-dependent mode-locking properties of the laser when the EDF length is fixed to be 1.5 m. The central wavelength, spectral width and pulse energy were measured using an optical spectrum analyzer and power meter. We adjusted the pumping power with a polarization controller to slightly less than the value at which the continuous wave (CW) spike appears. Furthermore, the dependences of the pulse energy and spectral width on the EDF length were investigated by varying the EDF and SMF28 lengths simultaneously; the net cavity dispersion was fixed to be 0.017 ps^2.

3. Results and discussion

To characterize the properties of the output pulse based on the net GVD of the laser, the net cavity dispersion was varied from –0.004 ps^2 to 0.027 ps^2 by changing the length of the SMF28 fiber. The maximum spectral width and pulse energy range were measured in the stably mode-locked region without CW spikes. The experimental results are shown in Figs. 3 and 4. In the near zero dispersion region, single pulse mode-locking was not achieved and multiple pulsing was observed with CW spikes in the spectral domain as shown in Fig. 4(a), meaning that the SWNT SA cannot support mode-locking in near zero dispersion due to low

#232601 - $15.00 USD Received 16 Jan 2015; revised 6 Mar 2015; accepted 6 Mar 2015; published 17 Mar 2015

modulation depth. When the net dispersion was 0.006 ps^2, a stably operated Gaussian-shaped single pulse was generated. As the net dispersion was incrementally varied from 0.006 $ps^2$to 0.017 ps^2, the spectral width, pulse energy, and central wavelength also increased. Figure 4(b) shows the spectrum at 0.017 ps^2-net dispersion. The dependencies of the spectral width and pulse energy on the net cavity dispersion are similar to those determined in [18]. The results also demonstrate that the operating wavelength can be controlled by adjusting the net cavity dispersion. For net cavity dispersions of between 0.017 and 0.027 ps^2, a mode-locked pulse could not be generated, whereas at 0.027 ps^2, a pulse with a 16-nm spectral width, steep edge, and central wavelength of 1570 nm was generated as shown in Fig. 4(c). This is due to the spectral filtering effect of the EDF and manifested in the limitation of further shifting the output pulse to a longer wavelength, where the limit in the obtainable center wavelength was approximately 1590 nm.

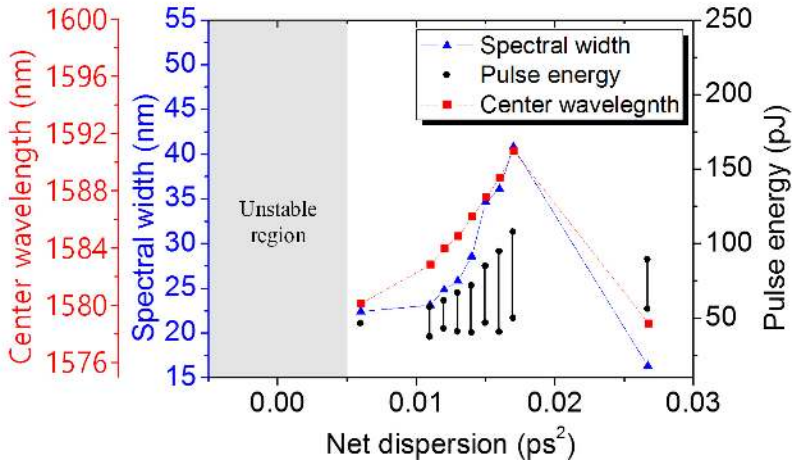

Fig. 3. Output pulse properties versus net cavity dispersion: central wavelength, spectral width(full width at half maximum; FWHM) and pulse energies (connected circle).

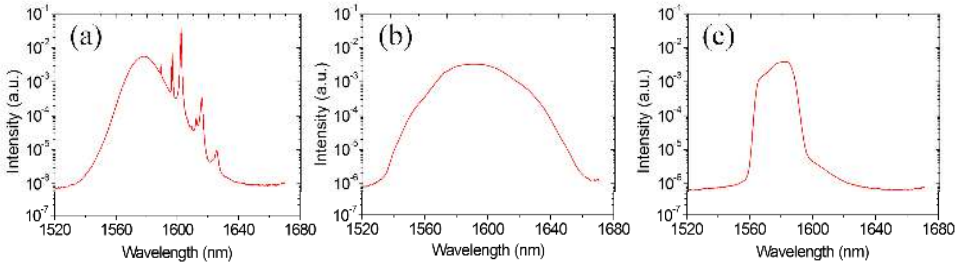

Fig. 4. Spectra of output pulses when the net cavity dispersion was (a) 0.004ps^2, (b) 0.017 ps^2, and (c) 0.027 ps^2.

In previous research, an unstable region occurs when the net dispersion of the SWNT-SA mode-locked laser approaches zero [22, 23]. In [24], Liu et al. demonstrated that as the spectral bandwidth increases, spectral filtering due to the finite gain bandwidth increases the loss experienced by the pulses. This effect creates instabilities that are due to low peak power, ultimately leading to unstable mode-locking. A laser operated in the L-band at a low average inversion has a flatter intrinsic net gain spectrum compared with that in the C-band [25]. Consequently, we could decrease the effect of spectral filtering, and thus, obtain the

#232601 - $15.00 USD Received 16 Jan 2015; revised 6 Mar 2015; accepted 6 Mar 2015; published 17 Mar 2015

ultrashort pulse with large spectral bandwidth at slightly positive net dispersion region even with a low modulation depth of 10%.

Figure 5 shows the EDF length dependent mode-locking properties in the stably mode-locked region. The net cavity dispersion is fixed to be 0.017 ps^2. We verified that stretched pulse is stably generated ifthe length of EDF is between 1.5 m and 2 m, and a shorter EDF produces a broader spectral width. This result was acquired with constant total cavity loss, but it is worth mentioning that with a slightly decreased cavity loss (by controlling the coupling ratio or the initial transmittance of the saturable absorber), the graph shifts to the right hand side, giving a broader spectral width at the same EDF length. The maximum spectral width we could obtain was limited to approximately 40 nm. If the SWNT-SA modulation depth is optimized, a much larger spectral width may be achieved. Therefore, it should be noted that not only the net dispersion but also the EDF length and total cavity loss are important parameters in designing the stretched pulse laser, given that the modulation depth is limited to a moderate degree.

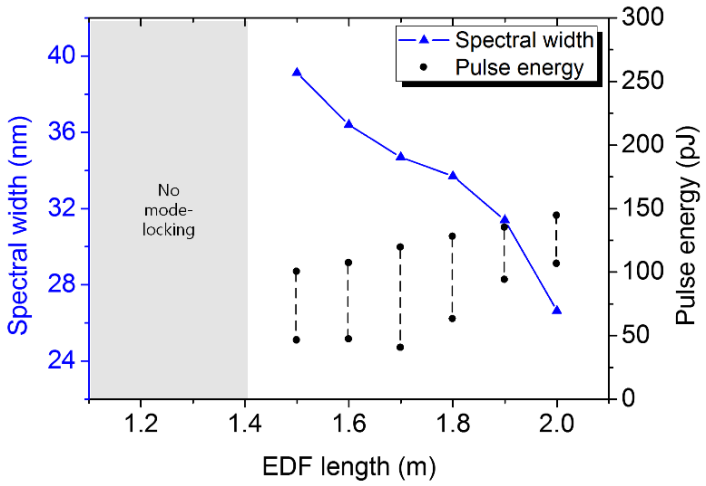

Fig. 5. The spectral width (FWHM) and pulse energy ranges (connected circles) versus EDF length.

Figure 6 shows the properties of the output pulse when the EDF length and net cavity dispersion are 1.5 m and 0.017 ps^2, respectively, for which the laser exhibits the largest spectral bandwidth and average output power of about 8 mW. The output pulse had positive chirp due to the relatively close displacement of the output coupler to the EDF, which was compensated externally using a SMF with negative GVD.A pulse duration of 110 fs and spectral width (full width at half maximum; FWHM) of 41 nm are measured. The time-bandwidth product (TBP) is 0.535. This value is slightly greater than 0.441, which is the TBP of transform-limited Gaussian pulses (transform-limited pulse duration 90 fs). This result is caused by uncompensated high-order dispersion. These results demonstrate an improvement over those of previous works [11, 16]. Figures 6(c) and 6(d) show the radio frequency (RF) signals of the output pulse. The RF signal measured at the fundamental repetition frequency with a 10-Hz resolution bandwidth had a signal-to-noise ratio of ~70 dB, which indicates that the pulse laser operates stably with low amplitude fluctuation and timing jitter.

#232601 - $15.00 USD Received 16 Jan 2015; revised 6 Mar 2015; accepted 6 Mar 2015; published 17 Mar 2015

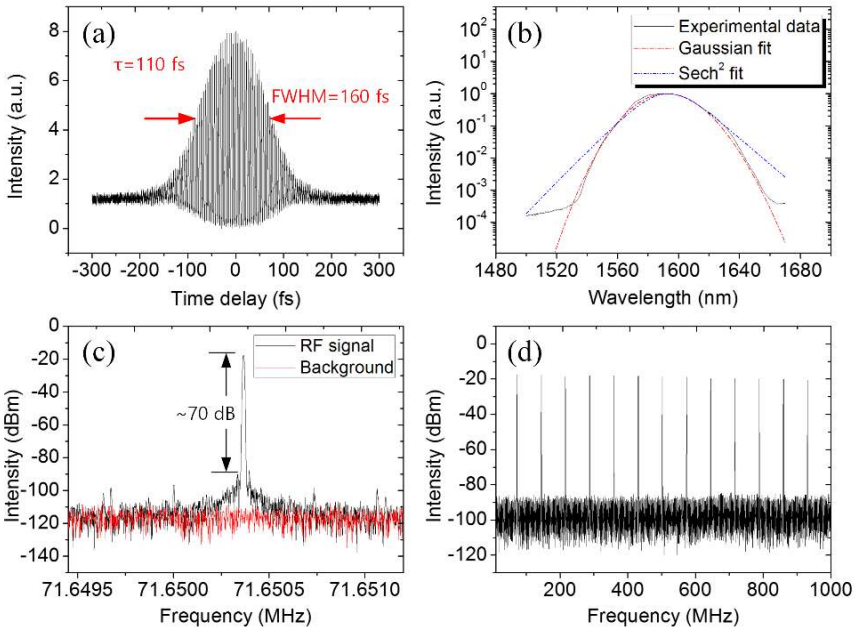

Fig. 6. Output properties of the laser when the length of the EDF and net cavity dispersion are 1.5 m and 0.017 $ps^{2,}$ respectively: (a) autocorrelation trace, (b) spectrum, (c) RF signal at the fundamental repetition frequency with a 10-Hz resolution bandwidth, and (d) RF signal over 1 GHz.

4. Conclusion

In this paper, we demonstrated the SWNT-SA based erbium-doped fiber ring laser operating in the L-band region. It was shown that the SWNTs produced by HiPCO process have almost same modulation depth at wavelength of 1560 nm and 1590 nm. Therefore, SWNT-SA was applicable for L-band pulse generation. In the design of erbium-doped fiber laser, the EDF length longer than 1.5 m was used and stretched pulse regime was employed, which let to generate the pulse with broad spectral width at the L-band region. Net dispersion dependent mode-locking properties were investigated. At the net dispersion of 0.017 ps^2, ultrashort pulse with 110 fs pulse duration and 41 nm spectral width was generated in L-band region. Despite of low modulation depth, the pulse was stably operated near zero dispersion. Proceeding from this fact, we conjecture that the flatter gain of EDF helps laser being stably operated near zero net dispersion. Further experimentation and numerical analysis considering the net gain profile and various modulation depth may be meaningful.

Acknowledgments

This work was supported by a grant from the National Research Foundation of Korea (NRF) funded by the Korean government (MSIP) (No. 2010-0017795) and under the framework of an international cooperation program managed by the National Research Foundation of Korea (No. 2013K2A1A2054170).

#232601 - $15.00 USD Received 16 Jan 2015; revised 6 Mar 2015; accepted 6 Mar 2015; published 17 Mar 2015